Article ID: 1006-8775(2017) 02-0202-08

THE IMPACTS OF INTERACTION OF A TYPHOON WITH THE MIDLATITUDE TROUGH ON ITS TRACK AFTER THE RECURVATURE

WANG Kai (王 凯)[1], CHEN Hua (陈 华)[2], WANG Jin-mei (王金梅)[2]
(1. Taizhou Meteorological Administration, Taizhou, Zhejiang 318000 China; 2. College of Atmospheric Science, Nanjing University of Information Science and Technology, Nanjing 210044 China)

Abstract: Three typhoon cases are selected to conduct a series of simulations that are initialized from sequential analyses. The results show that the forecast error in crucial area where a tropical cyclone (TC) interactes with the upstream trough is highly correlated to the track forecast error after the TC recurvature. Furthermore, sensitivity experiments confirm that the developments of the midlatitude downstream circulations and then the TC track after its recurvature are highly sensitive to the TC intensity and its location relative to the upstream trough, which can give an example or one way of sensitivity of the TC track to the TC-trough interaction. If the TC interacts with the upstream trough more strongly (e.g., the TC being intensified or getting closer to the upstream trough), the downstream circulations will be more meridional, thus the TC track will be more northerly and westerly; otherwise, the downstream circulations will be more zonal, and the TC track will be more southerly and easterly.

Key words: tropical cyclone; typhoon track; typhoon recurvature; midlatitude downstream circulations; upstream trough; PV gradient
CLC number: P444 **Document code:** A
doi: 10.16555/j.1006-8775.2017.02.008

1 INTRODUCTION

Because of complex physical processes and multiple scales, the numerical forecasting of extratropical transition (ET) of TCs is much more difficult than that of TCs or extratropical cyclones, and track prediction is one of its important issues. It is known that TC motion is governed by environmental steering flows. Therefore, the midlatitude circulations in which a TC is located mainly contribute to its movement during the ET process of the TC. Surely, a lot of complex factors can influence TC track, and many domestic scholars have studied this topic from many aspects[1–3].

Not only can the complex interactions during the ET process change the local atmospheric state around a TC, but also affect the atmospheric circulations over a large region. Especially, the downstream impacts are much more obvious[4]. The upstream trough plays a crucial role during the ET process and its downstream impact. Chen and Pan[5] indicated that the upstream trough can enhance the effects of upper-level outflow of a TC on the midlatitude jet. Röbcke et al.[6] found that TC location relative to the upstream trough is very important to the ET process and TC track prediction. A typical problem in the numerical prediction of ET is that sets of forecasts (including that of TC track) initialized from sequential analyses may differ much from one another. Chen and Pan [5] found that initial error can be transported to the midlatitude jet and be magnified there through the interaction between a TC and the upstream trough. Accordingly, we presume that the large differences at later forecasting stage might originate from the subtle differences in representation of the TC-trough interaction. Wu et al.[7] found that the sensitive area of the targeted observation for track forecasting of a TC in the midlatitudes is located in the upstream trough by taking into account the adjoint-derived sensitivity steering vector (ADSSV) and potential vorticity (PV). In this work, four TC cases are selected to conduct numerical experiments to verify the presumption above, and also to confirm the high sensitivity of the TC track after its recurvature to the interaction of the TC with the midlatitude systems. Furthermore, the related mechanisms will also be investigated. The objective metric developed by Archambault et al. [8] is employed to evaluate the strength of the TC-extratropical flow interaction. It should be noticed that the TC-trough interaction area includes numerous processes including the typhoon-trough interaction. Therefore, as an example, we only conduct those experiments to examine the

Received 2015-06-29; **Revised** 2017-04-11; **Accepted** 2017-05-15
Foundation item: International Cooperating Program of Science and Technology (2010DFA24650), National Natural Science Foundation of China (41175061)
Biography: WANG Kai, M.S., Research Assistant, primarily undertaking research on numerical simulation and urban climate.
Corresponding author: CHEN Hua, e-mail: huach@nuist.edu.cn

sensitivity of the TC track after its recurvature to its intensity and location relative to the upstream trough.

2 DATA AND METHODOLOGY

The datasets used in this work are the 6-hourly NCEP FNL reanalysis data with the resolution of 1°× 1° latitude-longitude and the best-track data from 1949 to 2010 from China Typhoon Center. The Weather Research and Forecasting Model (WRF) is employed. Four TC cases are Songda (2004), Nabi (2005), Choi-wan (2009) and Malakas (2010). They had the same characteristics, i.e., they all interacted with the upstream troughs while moving northward, and then were steered northeastward by the flows ahead of the troughs. At last they all transformed to extratropical cyclones.

For every TC case of Songda, Choi-wan and Nabi, we select 8 sequential times (at intervals of 6 hours) before the TC contacted with the upstream trough as the initial time of eight simulating experiments, and then select the crucial area where the TC interacted with the upstream trough (area A in Fig. 1), the upstream jet area (area B) and the subtropical high area (area C) as three influencing areas to respectively calculate their area-averaging root-mean-square forecasting errors of geopotential height in the eight experiments. The calculating time is a moment when the TC approached the upstream trough. For area A (also B), the calculating level is 200 hPa because the TC acted on the midlatitude flows at upper levels by the outflow before merging into them, while for area C it is 500 hPa.

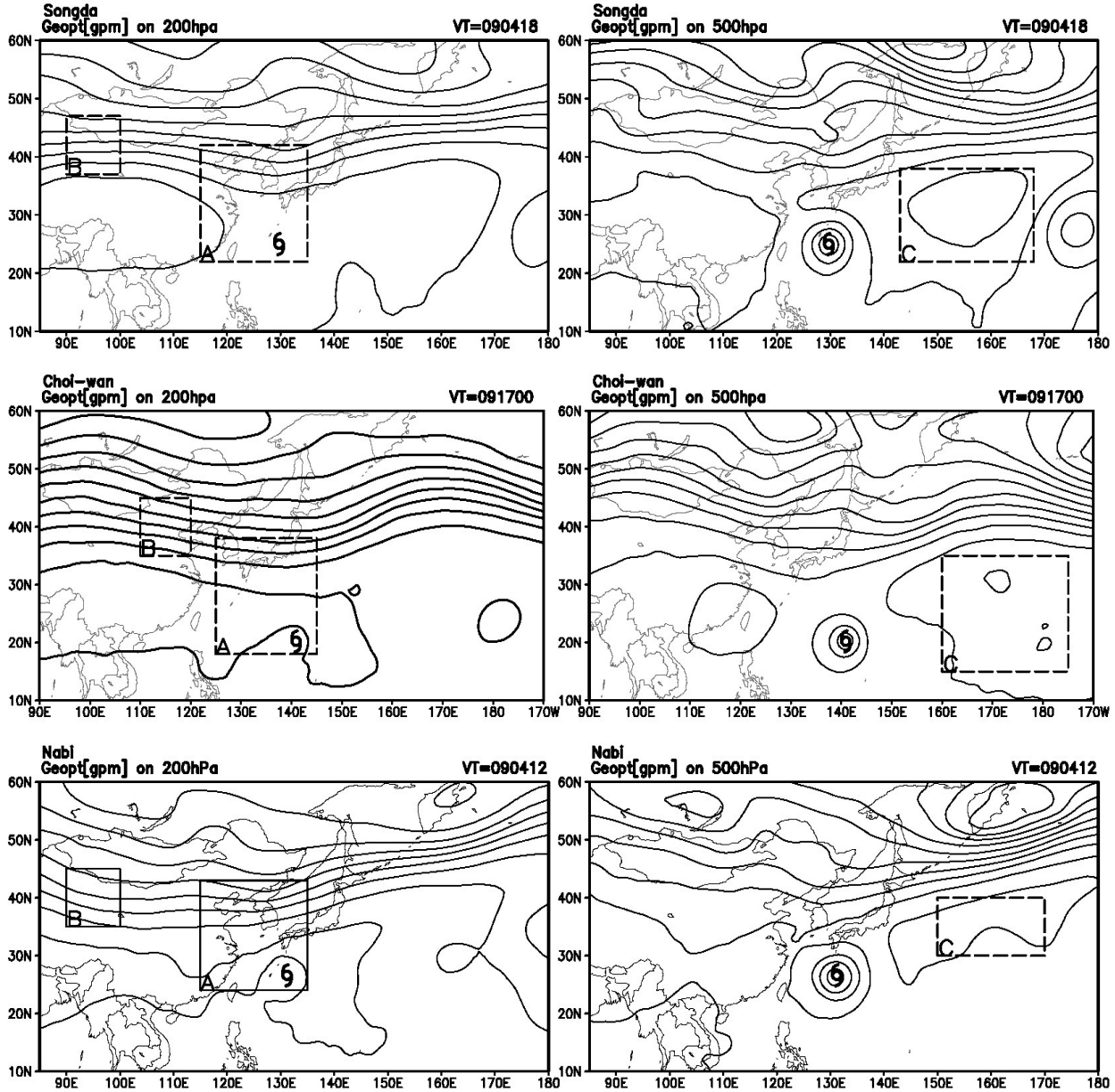

Figure 1. Influencing areas in every Typhoon case. Rectangles indicate area A for the TC-trough interaction, B for the upstream jet and C for the subtropical high respectively. Black contour lines are geopotential height analysis at 200 and 500 hPa. Typhoons are marked by a black symbol.

Root-mean-square forecasting error is defined as,

$$\sigma=\sqrt{\frac{\sum (F_i-G_i)^2}{n}}$$

Here, i indicates the grid point; n is sum of grid points in an area; F_i and G_i are forecasting value and analysis value respectively.

Next, we calculate the track forecasting errors in the eight experiments at a time after the TC recurved, and then calculate the correlation coefficients of them with root-mean-square forecasting errors of three influencing areas respectively. In addition, four sensitivity experiments and control experiment are designed for the Typhoon Malakas case. They all have the initial time of 0000 UTC 23. In the sensitivity experiments, the original typhoon is reremoved by the filter method proposed by Kurihara et al.[9]. Thereafter, we utilize the Bogus method of Wang et al.[10] to intensify or weaken the TC, or move the TC to the northwest or southeast, namely closer to or further away from the upstream trough. These experiments are respectively named as CONTROL, STRONG, WEAK, NORTHWEST and SOUTHEAST. The experiment designs are in Table 1.

Table 1. Description of all experiments.

Experiment	Description	Centre Pressure (hPa)	Location
CONTROL	The forecast is initialized from the analyses with no changes for the TC intensity and location.	985.939	141.1°E, 19.8°N
STRONG	The forecast is initialized with an intensified TC.	968.616	141.1°E, 19.8°N
WEAK	The forecast is initialized with a weakened TC.	1001.63	141.1°E, 19.8°N
NORTHWEST	The forecast is initialized with a TC that is removed closer to the upstream trough.	988.839	139.5°E, 22.37°N
SOUTHEAST	The forecast is initialized with a TC that is removed away from the upstream trough.	988.648	142.8°E, 18.32°N

3 THE ERRO R SOURCES OF TC TRACK FORECASTING AFTER THE RECURVATURE

3.1 *Songda*

The time at which root-mean-square errors are calculated is 1800 UTC 4 Septempber, and the sequential initial times of eight simulation experiments are 1800 UTC 31 August, 0000 UTC 1 September, 0600 UTC 1 September, 1200 UTC 1 September, 1800 UTC 1 September, 0000 UTC 2 September, 0600 UTC 2 September, and 1200 UTC 2 September. The sizes and locations of three influencing areas are shown in Fig.1. Songda recurved toward the northeast at 1200 UTC 6 September. Table 2 shows the result of correlation analyses for the Songda case. It should be known that there are six selected times after the recurvature, at each of which track prediction errors are calculated and correlation analyses are performed. We can find that the forecast errors of area A has significant correlation with the track forecast errors at each time after the TC recurvature. Area B shows low correlation, and area C shows significant correlation. It reveals that the upstream jet had no significant effects on the TC track, while the subtropical high had important effects. As Songda approached the midlatitude trough, the subtropical high was still strong and was located by west, thus its peripheral flows had important steering effects on Songda, even after the recurvature.

Table 2. The correlation analyses for track prediction errors after the recurvature with the root-mean-square errors of geopotential height in three influencing areas in the Songda case. Height forecasting errors are calculated at 1800 UTC 4 September. Track prediction errors are calculated six times respectively, and at every time, correlation analyses are performed for track errors with height errors. S refers to significant result and N insignificant result.

Calculating times of track errors	Correlation coefficient (Column 1 for area A; 2 for B; 3 for C)			*t*-test value (Column 1 for A; 2 for B; 3 for C)			Test results (Threshold t_α=2.45) (Column 1 for area A; 2 for B; 3 for C)		
12/07/09	0.707	−0.484	0.836	2.448	−1.355	3.730	S	N	S
18/07/09	0.721	−0.506	0.854	2.547	−1.436	4.021	S	N	S
00/08/09	0.742	−0.462	0.860	2.708	−1.275	4.135	S	N	S
06/08/09	0.824	−0.434	0.832	3.556	−1.179	3.679	S	N	S
12/08/09	0.823	−0.424	0.842	3.555	−1.148	3.829	S	N	S
18/08/09	0.841	−0.369	0.814	3.807	−0.971	3.435	S	N	S

3.2 *Choi-wan and Nabi*

In the Choi-wan case, the sequential initial times are 0000 UTC 13 September, 0600 UTC 13 September, 1200 UTC 13 September, 1800 UTC 13 September, 0000 UTC 14 September, 0600 UTC 14 September, 1200 UTC 14 September, and 1800 UTC 14 September. The calculating time of area errors is 0000 UTC 17 September. Area A shows significant correlation, while area B and C show low correlation (Table 3). In Nabi case, the initial times are 1200 UTC 30 August, 1800 UTC 30 August, 0000 UTC 31 August, 0600 UTC 31 August, 1200 UTC 31 August, 1800 UTC 31 August, and 0000 UTC 01 September, 0600 UTC 01 September. The calculating time of area errors is 1200 UTC 04 September. Also, area A shows significant correlation, while area B and C show low correlation (Table 4). Different from that in the Songda case, the subtropical high had no significant effects on the TC track in the two cases. In Fig.1, the subtropical high in the two cases was somewhat weak and was located by east, thus its peripheral flows had much weak effects on the TC.

Table 3. As in Table 2, but for Choi-wan case. The calculting time for area forecasting errors is 0000 UTC 17 September.

Calculating times of track errors	Correlation coefficient (Column 1 for area A; 2 for B; 3 for C)			*t*-test value (Column 1 for A; 2 for B; 3 for C)			Test results (Threshold t_α=2.45) (Column 1 for area A; 2 for B; 3 for C)		
12/19/09	0.765	−0.025	−0.461	2.911	−0.051	−1.274	S	N	N
18/19/09	0.790	−0.094	−0.475	3.154	−0.188	−1.321	S	N	N
00/20/09	0.750	−0.035	−0.434	2.776	−0.070	−1.180	S	N	N
06/20/09	0.706	−0.062	−0.376	2.443	−0.123	−0.993	N	N	N
12/20/09	0.711	−0.064	−0.308	2.475	−0.128	−0.792	S	N	N
18/20/09	0.743	−0.119	−0.333	2.717	−0.239	−0.866	S	N	N

Table 4. As in Table 2, but for the Nabi case. The calculating time for area forecasting errors is 1200 UTC 4 September.

Calculating times of track errors	Correlation coefficient (Column 1 for area A; 2 for B; 3 for C)			*t*-test value (Column 1 for A; 2 for B; 3 for C)			Test results (Threshold t_α=2.45) (Column 1 for area A; 2 for B; 3 for C)		
06/06/09	0.971	−0.704	0.258	9.868	−2.431	0.654	S	N	N
12/06/09	0.956	−0.698	0.251	8.000	−2.390	0.636	S	N	N
18/06/09	0.959	−0.668	0.217	8.270	−2.201	0.544	S	N	N
00/07/09	0.968	−0.677	0.172	9.375	−2.254	0.429	S	N	N
06/07/09	0.925	−0.690	0.159	5.983	−2.335	0.395	S	N	N
12/07/09	0.925	−0.699	0.239	5.953	−2.397	0.602	S	N	N

4 THE IMPACTS OF INTERACTION OF A TYPHOON WITH THE MIDLATITUDE TROUGH ON ITS TRACK AFTER THE RE-CURVATURE

Chen and Pan[5] found that the TC-trough interaction can transport initial error to the midlatitude jet and amplify it there. The correlation analyses above have verified significant correlation of track prediction errors after the TC recurvature with forecasting errors of the interaction area. As a result, it is indicated that slight differences in representation of the TC-trough interaction by sets of forecasts initialized from sequential analyses are amplified during the interaction, which leads to a large variability of ET forecasting (including TC track forecasting) at the later stage. The motion of a TC is mainly governed by the steering flow, thus its track after the recurvature is determined by the midlatitude downstream circulations. Many evidences verified that the complex interactions of a TC with the midlatitude systems (e.g., the upstream trough, the jet) during the ET process can not only change the local atmospheric state around the TC, but also affect the atmospheric circulations over a large region. Especially, the downstream impacts are much more obvious, which in turn leads to the alteration of TC track after the recurvature. There are likely two main methods by which a TC interacts with the midlatitude circulations [11-13]. One is that the TC outflow transports low PV (high θ) air to the midlatitudes, which may modify the upper-level structure in the extratropics, and lead to a strengthened downstream ridge (a steepened tropopause). The ridge in turn excites the Rossby waves propagating downstream and downward, thus changes the structure of upper-lower level circulations in the midlatitudes. The other is that through action at a distance, the circulations associated with the TC excite the Rossby waves on the upper-level PV gradients

associated with the jet before the PV anomaly of the TC meets with that of the jet. The Rossby waves will disperse on the PV gradients by the method discussed by Simmons and Hoskins [14]. According to the PV thinking, the genesis and propagation of the Rossby waves are just the process in which initial disturbances are excited and propagated on PV gradients [15]. Therefore, under the effects of ET system, the strength of the midlatitude downstream circulations is determined by two factors. One is the strength of the TC outflow's transporting low-PV air downstream, and the other is the strength of PV gradient being disturbed in the midlatitude jet.

Figure 2 is dynamic tropopause maps (θ map on 2 PV surface) in the control and all the sensitivity experiments at the forecast valid time of 72 h. In NORTHWEST, the bogus TC was removed to the north artificially, and then the outflow was destroyed to some extent. As a result, the outflow was even weaker than that in CONTROL in the following simulation (not shown). The stronger downstream baroclinic developments in NORTHWEST could be attributed to earlier and stronger disturbance of the PV gradient by the TC. Because of this, Fig.2 does not include a dynamic tropopause map in NORTHWEST. If the TC intensifies or is removed closer to the upstream trough, the downstream high-θ area (brown and bright red areas) that denotes the low PV outflow region expands distinctly, and the field extends meridionally more intensely. Otherwise, if the TC is weakened or removed away from the upstream trough, the high-θ area decreases, and is located by west; moreover, the field develops to be more zonal and gentle. It reveals that, if the TC intensifies or is removed closer to the upstream trough, the process in which the TC outflow transports low-PV air to the midlatitudes is strengthened, and the disturbance of the PV gradient by the TC is also strengthened; otherwise, the results will be reversed.

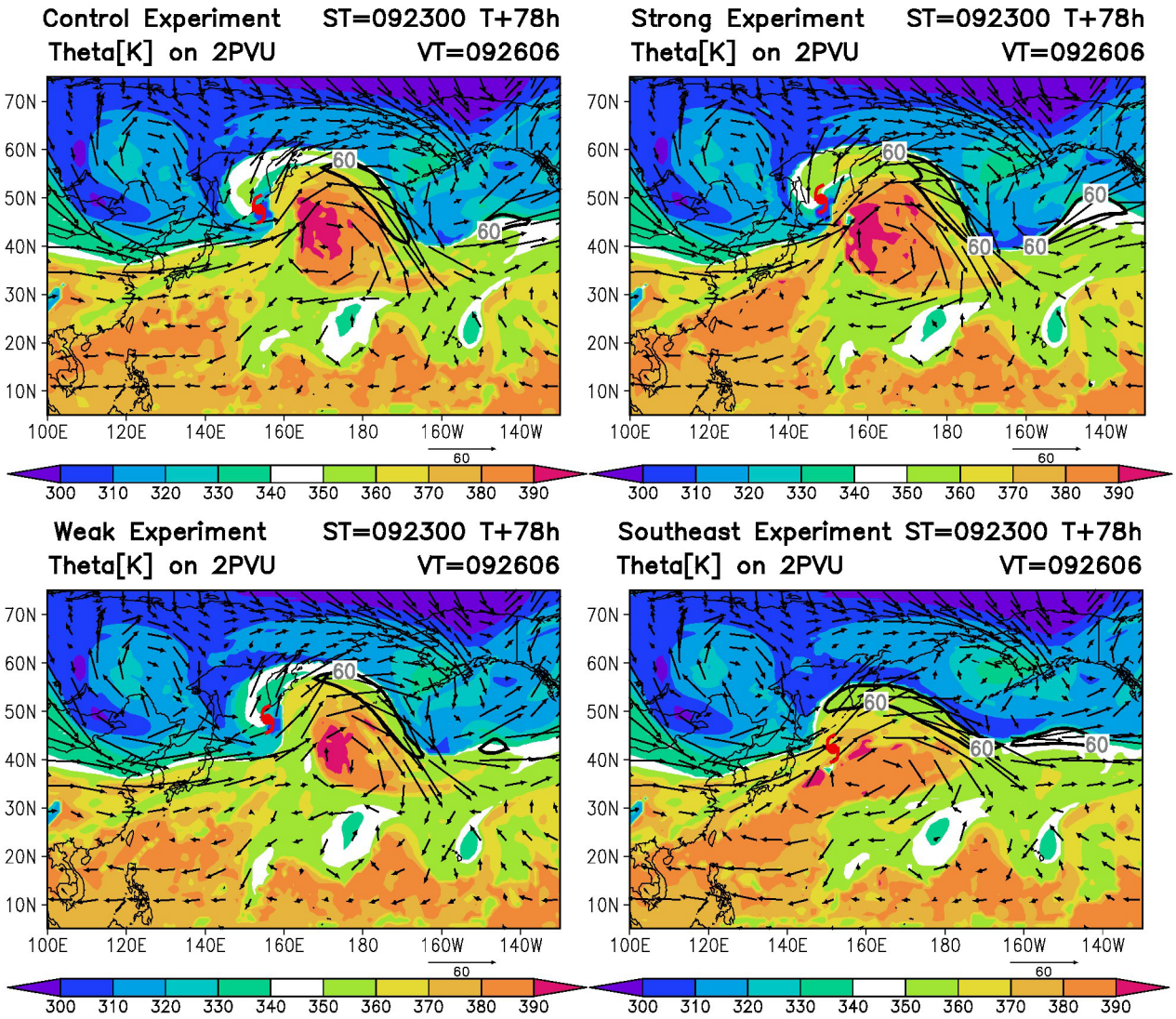

Figure 2. θ maps on dynamic tropopause (2 PV surface) in the sensitivity experiments and the control experiment at forecast time of 78 h. Black arrows are wind vectors. The strongest jet regions where wind speeds are >60 m s^{-1} are outlined by black, bold and solid lines.

Archambault et al.[8] indicated that the TC outflow impinging the midlatitude jet is the critical process that induces downstream Rossby wave growth although many features of a TC contribute to its interaction with the midlatitude flow. This process actually includes the role of diabatic heating: "low upper-tropospheric PV air that arises from the vertical redistribution of PV by diabatic heating is then advected poleward by the diabatically driven divergent outflow." Therefore, the negative PV advection caused by the TC divergent outflow is employed as an objective metric to measure the strength of the TC interacting with the midlatitude flow. The detailed steps to calculate "the TC-extratropical flow interaction metric" can be found in the work of Archambault et al.[8]. A brief description is given as follows:

1) the point and time of the maximum TC-extratropical flow interaction (i.e., the maximum 250–150 hPa layer-averaged negative PV advection by the irrotational wind) surrounding TC recurvature are identified;

2) a spatial average of the 250 –150 hPa layer-averaged PV advection by the irrotational wind is computed for a 15°× 15° domain centered on the point of maximum interaction;

and 3) a temporal average of the spatially-averaged PV advection by the irrotational wind is computed for a 48-h period centered on the time of maximum interaction.

In this work, the objective metric is used to evaluate the strength of the TC-extratropical flow interaction in every simulation experiment, so as to detect the impacts of the TC intensity and its location relative to the upstream trough on the interaction. The calculated results (Table 5) show that the interactions in STRONG and NORTHWEST are strengthened, while those in WEAK and SOUTHEAST are weakened. In general, if the TC intensifies or is removed closer to the upstream trough, the TC-extratropical flow interaction is strengthened because the TC outflow is strengthened and the outflow could transport low-PV air to the midlatitudes more strongly with the assistance of southwestern flows on the eastern flank of the trough. As a result, the PV gradient in the downstream region is enhanced. Moreover, the TC disturbs the PV gradient more strongly because the circulations associated with the TC are intensified and the TC is closer to the midlatitude flows. From the PV perspective, it can be foreseen that the downstream baroclinic developments will be intensified. If the TC is weakened or removed away from the upstream trough, the opposite would happen. Sensitivity experiments show that slight alterations of TC intensity and location relative to the upstream trough can result in large variations of the midlatitude downstream circulations, and the TC track in turn varies. The comparison of 200 hPa height forecasts at 78 h between the control experiment and the sensitivity experiments (Fig.3) and the comparison among best-track and simulated tracks in all experiments (Fig.4) indicate that, if a TC interacts with the upstream trough strongly (e.g., the TC being intensified or being closer to the upstream trough), the midlatitude downstream circulations are strengthened and more meridional, especially, the western flank of the ridge just downstream of the TC protrudes distinctly. Corresponding to the downstream developing circulation, the TC track after the recurvature will be more northerly and westerly; otherwise, the downstream circulations will be weakened and more zonal, the TC track being more southerly and easterly. In conclusion, slight differences in simulating the TC-trough interaction by sets of forecasts initialized from sequential analyses lead to distinct variations of the midlatitude downstream circulations, thus changing the steering flows after the TC recurvature and in turn resulting in the large variability of TC track.

Table 5. The TC-extratropical flow interaction metric in each experiment (PVU day^{-1}, 1 PVU$=10^{-6}$ Km^{2}kg^{-1} s^{-1}).

Experiments	Maximum Interaction	The Point of Maximum Interaction	The Time of Maximum Interaction	Interaction Metric
CONTROL	–106.816	(139.635,45.3684)	9–25–00	–5.617001111
STRONG	–95.9354	(145.032,49.0331)	9–25–06	–5.849923222
WEAK	–130.861	(140.714,46.1217)	9–25–00	–5.016001
NORTHWEST	–92.737	(140.714,46.1217)	9–24–18	–6.483623444
SOUTHEAST	–77.0656	(136.397,43.0479)	9–25–06	–5.268826667

5 CONCLUSIONS

Simulating experiments and correlation analyses for four typhoon cases in this work show significant correlation of track prediction error after the TC recurvature with forecasting error in areas where a TC interacted with the upstream trough. The subtropical high area shows significant correlation in some cases, but the upstream jet area does not show any correlation. As to physical mechanisms, the complex interactions of a TC with the midlatitude systems (e.g., the upstream trough, the jet) can affect the midlatitude downstream circulations, thus changing the steering flows after the TC recurvature, and in turn influencing the TC track. If

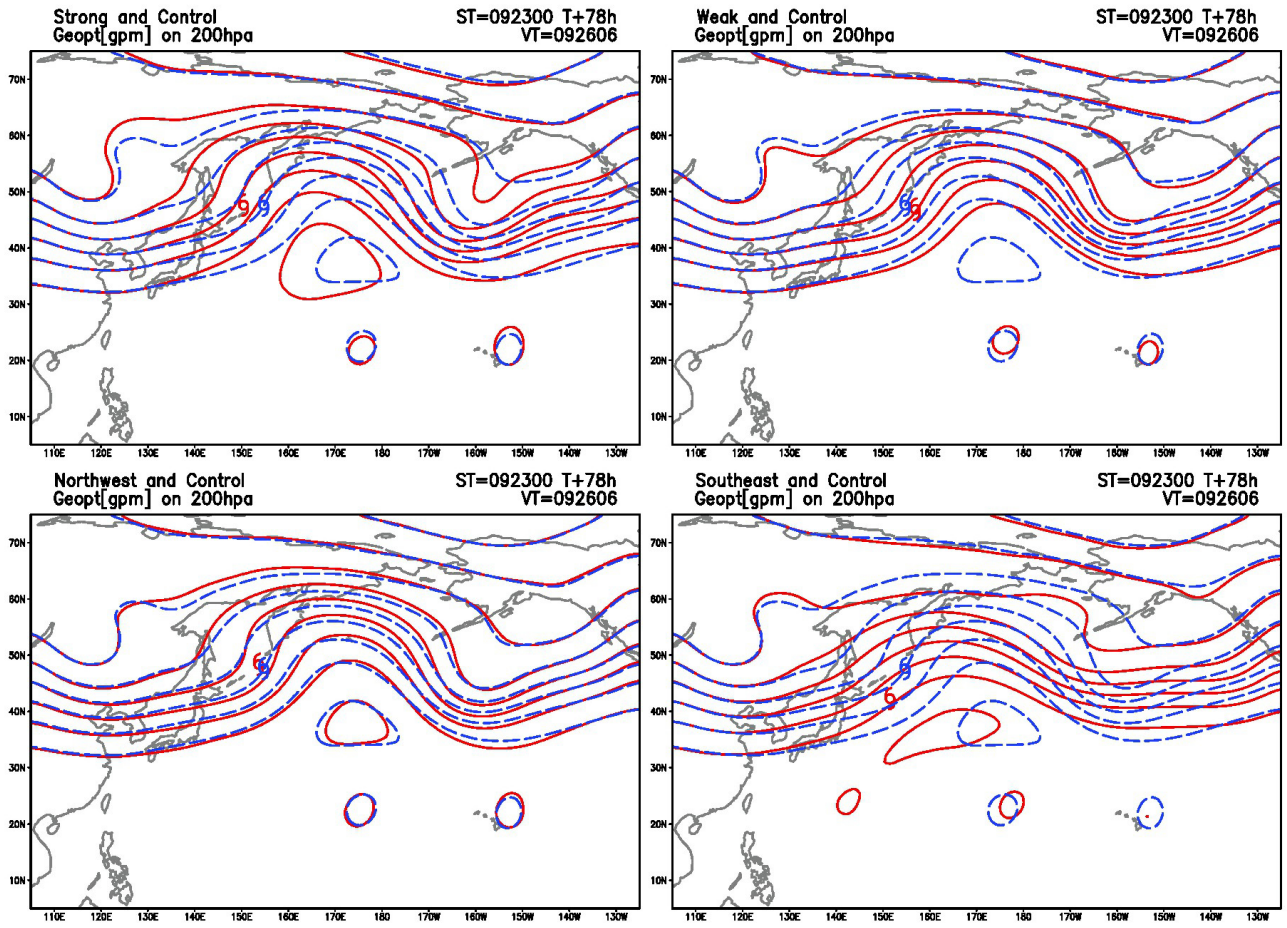

Figure 3. Forecasts of 200 hPa geopotential height in all experiments at the forecast time of 78 h. Red contour lines are forecasts of the sensitivity experiments, and blue contour lines are forecasts of the control experiment. Malakas is marked by a red symbol.

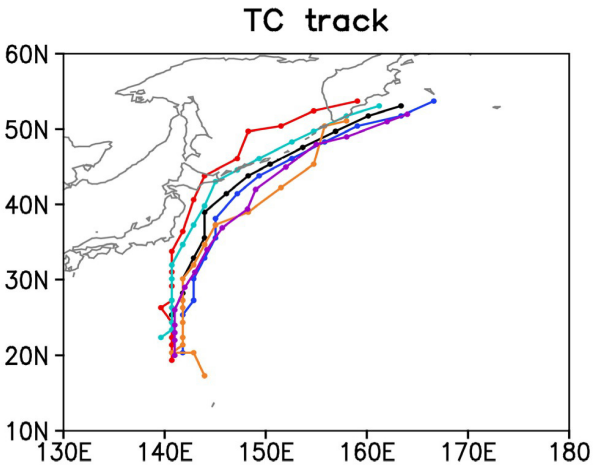

Figure 4. Best-track and simulated tracks in all experiments for Typhoon Malakas. Black line is the track in CONTROL; Red line is the track in STRONG; Blue line is the track in WEAK; Cyan-blue line is the track in NORTHWEST; Brown line is the track in SOUTHEAST; Purple line is best-track.

the TC-trough interaction is stronger (e.g., the TC being intensified or being closer to the upstream trough), the TC outflow transports low-PV air to the midlatitudes more strongly, which leads to the enhanced PV gradient in the downstream region, and the disturbance of the PV gradient by the TC is also strengthened. As a result, the midlatitude downstream circulations are strengthened and more meridional, and the TC track after the recurvature will be more northerly and westerly; otherwise, the downstream circulations are weakened and more zonal, and the TC track will be more southerly and easterly. Generally, besides the typhoon-trough interaction, numerous processes exist in the TC-trough interaction area. Therefore, the sensitivity experiments only give an example or one way by which the TC-trough interaction influences the TC track. Based on these results, it can be concluded that slight differences in simulating the TC-trough interaction by sets of forecasts initialized from sequential analyses are amplified during the interaction, and then the amplified differences lead to distinct variations of the midlatitude downstream circulations. Thus the steering flows after the TC recurvature are changed, which in turn results in the large variability of TC track. If the subtropical high is strong and its location is more westerly, it has distinct effects on the recurvature of a TC and its track after the recurvature.

Numerical prediction of ET is difficult all the time, and track prediction is an important issue of it. The complex TC-extratropical flow interaction often occurs during ET process, and becomes one of the most important reasons of ET being a difficult numerical forecast issue. This work reveals the characteristics of the TC track during ET process by studying the TC-trough interaction. The results can be helpful to understanding the machanisms of the TC-extratropical flow interaction and the interaction influencing TC track. Moreover, these results can be taken as track predictors after a TC moves to the midlatitudes for operational departments, and promote the accuracy of TC track prediction. Operational departments can determine the TC track trend after a TC moves to the midlatitudes according to the phasing of the TC with the midlatitude flows and the TC intensity.

REFERENCES:

[1] WANG Dong-fa, YU Hui, ZHONG Yuan, et al. Factors affecting the track of tropical cyclones after landfall in eastern China [J]. J Trop Meteorol, 2007, 13(2): 185-188.

[2] FEI Jian-fang, LI Bo, HUANG Xiao-gang, CHENG Xiao-ping. On the relationships between the unusual track of Typhoon Morakot (0908) and the upper westerly trough [J]. J Trop Meteorol, 2012,18(2): 187-194.

[3] LIN Zhi-qiang, BIANBA Zha-xi, WEN Sheng-jun, et al. The objective clustering of tropical storms tracks over the bay of Bengal [J]. J Trop Meteorol, 2013, 29(6): 973-983 (in Chinese).

[4] JONES S C, HARR P A, ABRAHAM J, et al. The extratropical transition of tropical cyclone: Forecast challenges, current understanding, and future directions [J]. Wea Forecast, 2003, 18(6): 1052-1092.

[5] CHEN Hua, PAN Wei-yu. Denial experiments of targeted observations for extra-tropical transition of hurricane Fabian: Signal propagation, the interaction between Fabian and mid-latitude flow, and observation strategy [J]. Mon Wea Rea, 2010, 138(8): 3324-3342.

[6] RÖBCKE M, JONES S C, MAJEWSKI D. The extratropical transition of Hurricane Erin (2001): A potential vorticity perspective [J]. Meteorol Zeitschr, 2004, 13(6): 511-525.

[7] WU C C, CHEN S G, CHEN J H, et al. Interaction of Typhoon Shanshan (2006) with the midlatitude trough from both adjoint-derived sensitivity steering vector and potential vorticity perspectives [J]. Mon Wea Rev, 2009, 137(3): 852-862.

[8] ARCHAMBAULT H M, BOSART L F, KEYSER D, et al. A climatological analysis of the extratropical flow response to recurving Western North Pacific Tropical Cyclones [J]. Mon Wea Rev, 2013, 141(7): 2325-2346.

[9] KURIHARA Y, BENDER M R, ROSS R J. An initialization scheme of hurricane models by vortex specification [J]. Mon Wea Rev, 1993, 121(7): 2030-2045.

[10] WANG Guo-min, WANG Shi-wen, LI Jian-jun. A bogus typhoon scheme and its application to a movable nested mesh model [J]. J Trop Meteorol, 1996, 12(1): 9-17 (in Chinese),.

[11] KLEINSCHMIDT E. Über den aufbau und entstehung von Zyklonen II [J]. Meteorol Rundsch, 1950, 3 (5): 54-61.

[12] DAVIS, C A, STOELINGA M T, KUO Y H. The integrated effect of condensation in numerical simulations of extratropical cyclogenesis [J]. Mon Wea Rev, 1993, 121(8), 2309-2330.

[13] BISHOP C H, THORPE A J. Potential vorticity and the electrostatics analogy: Quasigeostrophic theory [J]. Quart J Roy Meteorol Soc, 1994, 120(517): 713-731.

[14] SIMMONS A J, HOSKINS B J. Downstream and upstream development of unstable baroclinic waves [J]. J Atmos Sci, 1979, 36(7): 1239-1254.

[15] HOSKINS B J, MCINTYPE M E, ROBERTSON A W. On the use and significance of isentropic potential vorticity maps [J]. Quart J Roy Meteorol Soc, 1985, 111 (470): 877-946.

Citation: WANG Kai, CHEN Hua and WANG Jin-mei. The impacts of interaction of a typhoon with the midlatitude trough on its track after the recurvature [J]. J Trop Meteorol, 2017, 23(2): 202-209.